

On the relative abundances of Cavansite and Pentagonite

Bhalchandra S. Pujari

Department of Scientific Computing Modeling & Simulation, Savitribai Phule Pune University, Pune 411007, India.

E-mail: bspujari@scms.unipune.ac.in

Sagar Gehlot

Department of Scientific Computing Modeling & Simulation, Savitribai Phule Pune University, Pune 411007, India.

Mihir Arjunwadkar

Department of Scientific Computing Modeling & Simulation, Savitribai Phule Pune University, Pune 411007, India.

Dilip G. Kanhere

Department of Scientific Computing Modeling & Simulation, Savitribai Phule Pune University, Pune 411007, India.

Raymond A. Duraiswami

Department of Geology, Savitribai Phule Pune University, Pune 411007, India.

December 2023

Abstract. Cavansite is a visually stunning blue vanadosilicate mineral with limited occurrences worldwide, whereas Pentagonite is a closely related dimorph with similar physical and chemical properties, yet is extremely rare compared to Cavansite. The reasons behind Pentagonite's exceptional rarity remain largely unknown.

In this study, (a) density functional theory (DFT) is utilized to investigate the electronic structures of Cavansite and Pentagonite at ground state and finite pressures; (b) a two-state Boltzmann probability model is then employed to construct a comprehensive phase diagram that reveals the abundance of each species across a wide range of pressure and temperature conditions; and (c) dehydration characteristics of these two minerals are explored.

The present analysis reveals the key factors that contribute to the relative scarcity of Pentagonite, including differences in structural arrangement and electronic configurations between the two minerals. Specifically, it shows that (a) because of the peculiar arrangements of SiO_4 polyhedra, Cavansite forms a compact structure (about 2.7% less in volume) resulting in lower energy; (b) at a temperature of about 650K only about 1% Pentagonite can form; (c) vanadium induces a highly localized state in both of these otherwise large-band-gap insulators resulting in an extremely weak magnetic

phase that is unlikely to be observed at any reasonable finite temperature; and (d) water molecules are loosely bound inside the microporous crystals of Cavansite and Pentagonite, suggesting potential applications of these minerals in various technological fields.

Keywords: Zeolites, Cavansite, Pentagonite, Electronic structure, Relative abundance, Water, Geophysics

1. Introduction

Since its discovery[1] in the 1960s, Cavansite has been a highly coveted mineral due to its spectacular greenish-blue appearance. It is found in clusters of acicular crystals, with individual crystals being sub-millimeter in size. Pentagonite, though chromatically similar, is known for the twining that leads to a near-five-fold-symmetrical structure giving it its name [2, 3]. Being dimorphs, both have the same chemical formula – $\text{Ca}(\text{VO})\text{Si}_4\text{O}_{10}\cdot 4\text{H}_2\text{O}$ – and both are orthorhombic crystals with Pentagonite having slightly larger (by about 2% in volume) unit cell. The blueish color of both the minerals is attributed to vanadium atoms [4]. The other common interesting structural character of these dimorphs is the presence of large cavities in their atomic structure due to tetrahedral-pyramidal arrangements of vanadosilicate complexes. Sheets of SiO_4 are intertwined in a maze that accommodates calcium and vanadium atoms. In fact, these are the only known naturally occurring microporous vanadosilicates [5]. The resulting tunnels are naturally occupied by water and may be dehydrated at higher temperatures [6, 7]. Such materials are of technological importance due to their ion-exchange, catalytic or sorption applications. Because vanadium in these complex structures can be in multiple oxidation states they are expected to show catalytic activity; specifically, for selective partial oxidation of ethanol at elevated temperatures [8]. Interestingly, Cavansite was also investigated for bioavailability of vanadium for nitrogen fixation reaction carried out by certain bacteria where it was shown that bacteria may extract vanadium from Cavansite and may incorporate it into cellular biomass [9, 10].

Although first discovered in Oregon, USA, arguably best samples of these dimorphs are known to originate from Pune (formerly Poona), India [6, 7]. Worldwide, these minerals are known to be found at ten locations corresponding to only four basaltic planes; see Table A1. This table, wherever possible, also describes the associated minerals in the corresponding lava flows and shows that the two minerals are found among the upper flows of pahoehoe-type lava. (Unlike the aa-type flow, a pahoehoe-type lava flow is characterized by a relatively smooth surface.) The two minerals are formed inside cavities or brecciated surfaces. We also note that there are at least three sites where Cavansite and Pentagonite co-occur, and whereas Pentagonite is never found without Cavansite, the converse is not true. This gives a clear indication that Cavansite is significantly more abundant than Pentagonite. Unfortunately, quantitative

field measurements of their relative abundances are absent in field studies due to the rarity of these minerals. It has been noted, however, that it is nearly impossible to find reasonably large clusters of Pentagonite [11]. Therefore, considerable uncertainty remains about the nature of the formation processes of Cavansite and Pentagonite. That they can be found at the same location suggests that the chemical and physical environments responsible for their formation may be similar. It has been noted that their mineral associations and modes of occurrence are often similar [1]. Yet, Pentagonite remains significantly rarer.

In this study, density functional theory (DFT) calculations have been used primarily to explore why Pentagonite may be so rare. Formation energies of these minerals deduced thus, and the resulting phase diagram of their relative abundances, suggest why Cavansite remains dominant in the field. It may be noted that there have been no previous electronic structure investigation on these minerals.

2. Computational Details

DFT calculations were performed using the plane-wave basis set and within the Perdew-Burke-Ernzerhof (PBE) generalized gradient approximation [12], using Quantum ESPRESSO [13]. To ensure accuracy, the latest curated pseudopotentials [14, 15, 16] compiled by Materials Cloud [17, 18] have been used. Full unconstrained and spin-polarized unit cell optimizations were carried out starting from experimentally reported unit cells consisting of four chemical formula units, resulting in total of 116 atoms. To ascertain accuracy further, a rather high kinetic-energy cutoff of 950 eV was used for the plane wave basis set, and an automatic $3 \times 3 \times 3$ Monkhorst-Pack grid was used to sample the k -space during unit cell optimizations. For subsequent non-self-consistent calculations, a finer $6 \times 6 \times 6$ grid was used, and for band structure calculations, 30 k -points were used along each symmetry line in Brillouin zone. Finally, DFT-D3 treatment of Grimme et al. [19] was used to account for van der Waals correction which, as it turns out, plays a vital role in determining lattice structures; this is detailed later in this paper.

3. Results and discussion

3.1. Electronic structure

Fig. 1 shows the fully-optimized unit cells of Cavansite and Pentagonite. These are computed using full spin-polarized calculations as warranted by the presence of a transition element; i.e. Vanadium.

As there are four vanadium atoms, there can be four possible magnetic configurations: one ferromagnetic and three antiferromagnetic. Fig. 2 shows the schematics of the three antiferromagnetic phases. The ferromagnetic phase (i.e., all moment pointing in the same direction) is not shown. These four calculations have been performed by first initiating appropriate moments on the vanadium atoms and then fully relaxing the unit cell.

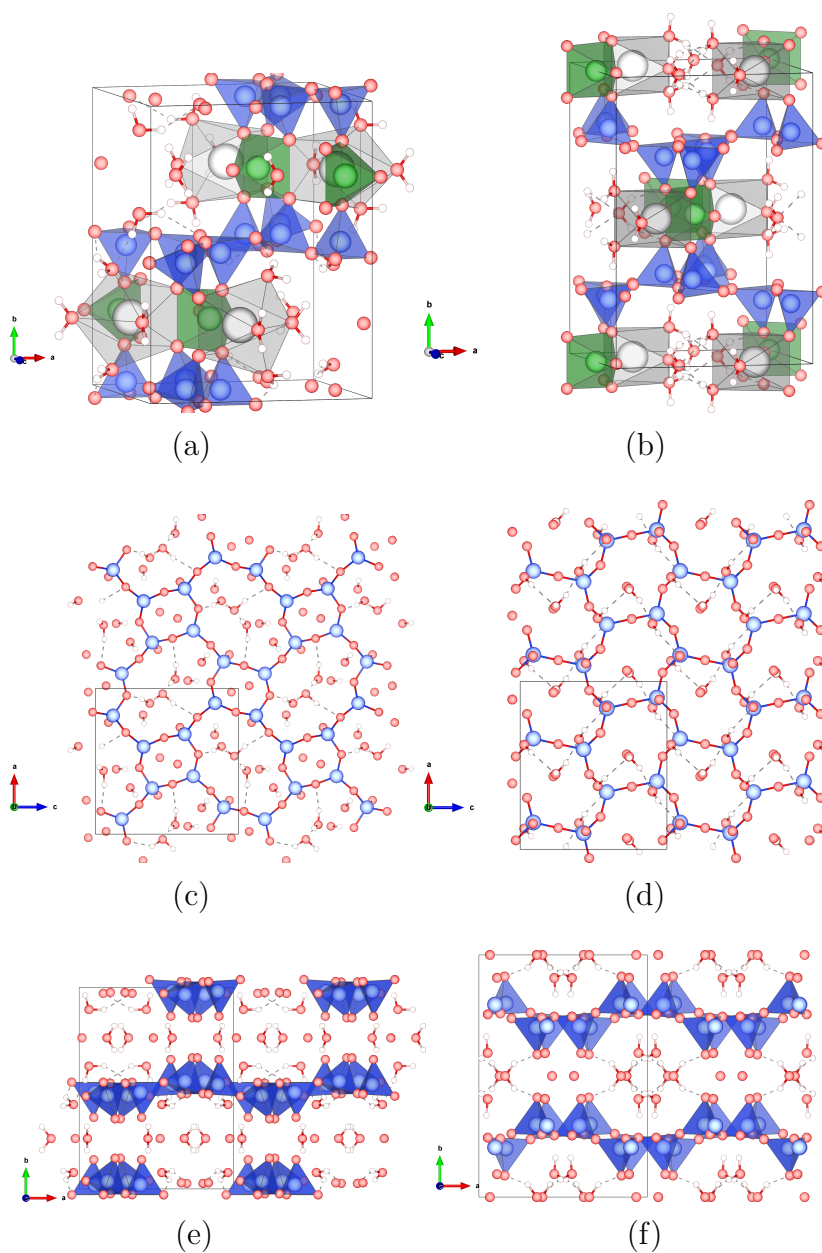


Figure 1. The unit cell views of Cavansite (left panel) and Pentagonite (right panel). The silicon atoms are in blue, oxygen atoms in red, calcium atoms in gray, vanadium atoms in green while hydrogen atoms are shown in white color. The polyhedra have same color themes. (a) and (b) are full unit cell structure shown at a visually convenient angle. For better understanding of underlying silicate framework we hide vanadium and calcium atoms in the following sub-figures. (c) and (d) show the ‘top view’ (along **b** axis) without the polyhedra, highlighting the ring-like structures of silicate sheets. Similar view along the **c** axis (which includes the polyhedra for better understanding) is shown in (e) and (f) for Cavansite and Pentagonite respectively.

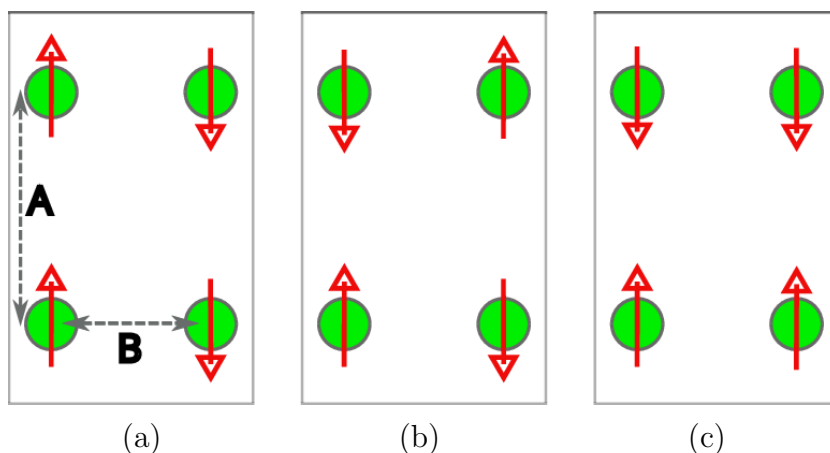


Figure 2. A simplistic schematic of three types of antiferromagnetic configurations. The four vanadium atoms are arranged in a parallelogram of sides A and B . For Cavansite $A = 6.88\text{\AA}$ and $B = 5.54\text{\AA}$, while for Pentagonite $A = 8.82\text{\AA}$ and $B = 4.42\text{\AA}$.

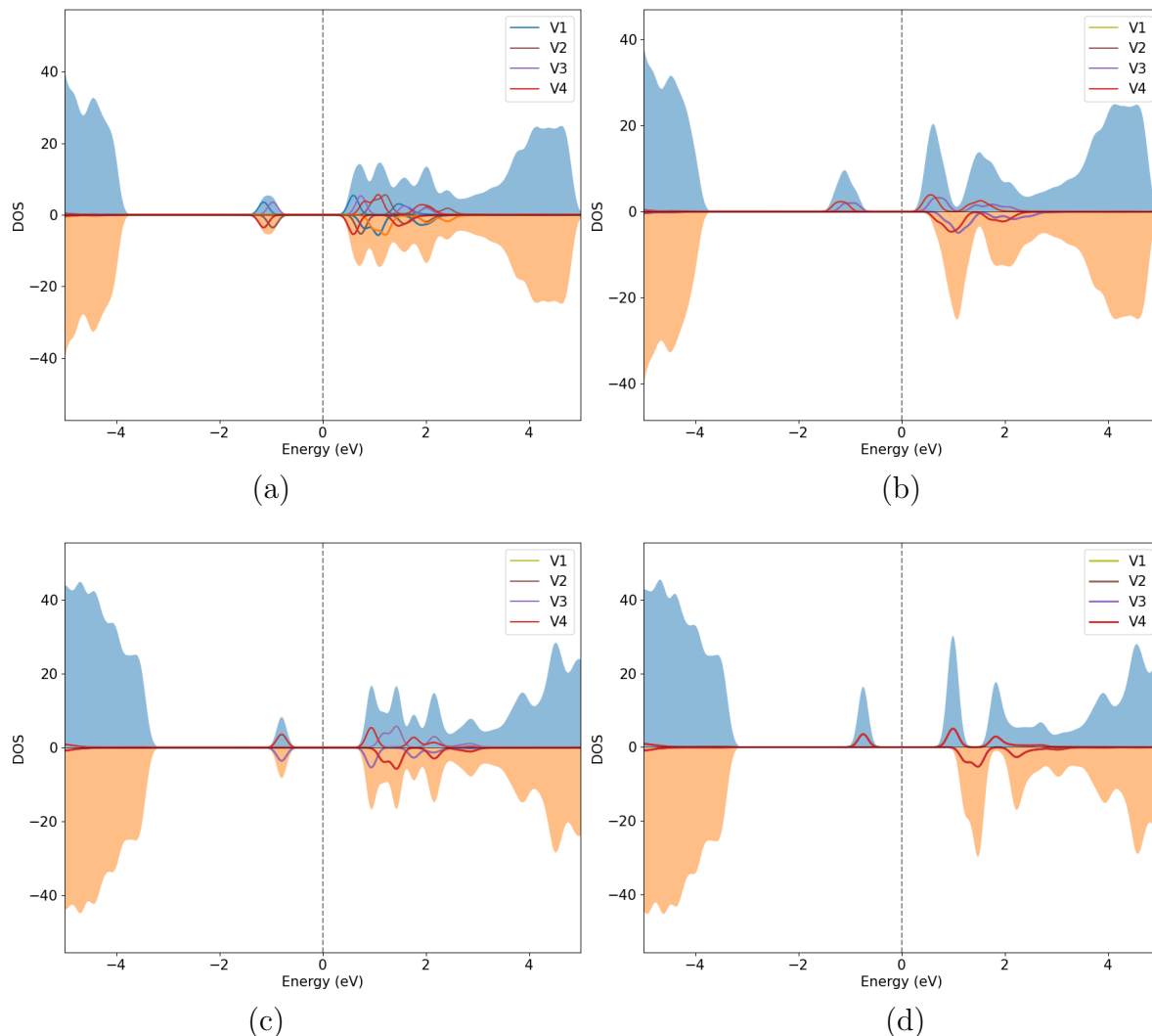


Figure 3. Total (shaded) as well as projected (lines) density of states for Cavansite; (a) antiferromagnetic and (b) ferromagnetic. (c) and (d): the same for Pentagonite. For the sake of visualization the down spin channel is shown with negative values.

	Present study	Experiment [2]	Experiment [20]
Cavansite	$a = 9.94\text{\AA}$ $b = 12.94\text{\AA}$ $c = 9.76\text{\AA}$ $V = 1256.19\text{\AA}^3$	$a = 9.792\text{\AA}$, $b = 13.644\text{\AA}$ $c = 9.629\text{\AA}$ $V = 1286.45\text{\AA}^3$	$a = 9.794\text{\AA}$, $b = 13.670\text{\AA}$ $c = 9.643\text{\AA}$ $V = 1291.1\text{\AA}^3$
Pentagonite	$a = 10.09\text{\AA}$ $b = 14.48\text{\AA}$ $c = 8.84$ $V = 1291.19\text{\AA}^3$	$a = 10.386\text{\AA}$ $b = 14.046\text{\AA}$ $c = 8.975\text{\AA}$ $V = 1309.29\text{\AA}^3$	$a = 10.376\text{\AA}$ $b = 14.062\text{\AA}$ $c = 8.984\text{\AA}$ $V = 1310.8\text{\AA}^3$

Table 1. Comparison of lattice parameters obtained from the present study and available experimental measurements.

For both the minerals, the optimized unit cells for all the four types of configurations are numerically identical up to three decimal places, although their energies differ as will be seen later. The unit cells are orthorhombic with the cell parameters as given in the Table 1. The table also shows the comparison of results of the present study with two experimental results. That the Pentagonite unit cell is 2.7% larger in volume than Cavansite is consistent with the experimental findings. The ground state for both the minerals is an antiferromagnetic phase depicted in Fig. 2(a), where localized moments on the vanadium atoms arranged in such a way that the nearest vanadium atoms are antiferromagnetically coupled while the next-nearest ones are ferromagnetically coupled. The magnetic moment on each atom is approximately $0.667\mu_B$ due to partial occupancy of d -orbitals. The electronic density of states are shown in Fig. 3 together with the contributions of the vanadium atoms. The left panel of the figure shows the density of states corresponding antiferromagnetic phase of Cavansite (top) and Pentagonite (bottom), and the right panel shows the same for ferromagnetic phase. The reader may notice highly localized d -states at ~ 1.3 eV arising from vanadium atoms as a mid-gap state in an otherwise large band gap (~ 4.6 eV) for all the cases. The differentiating factor between the two minerals is that for Pentagonite the contribution from all the four vanadium atoms is degenerate in the mid-gap state while for Cavansite the pairs of nearest neighbors are degenerate and there is a marginal shift between the two pairs. This can be attributed to larger separation of next nearest neighbors; i.e., 6.88\AA for Cavansite against 8.82\AA for Pentagonite (see Fig. 2) resulting in a weaker coupling.

Although the magnetic coupling among the vanadium atoms appears stronger in Cavansite than in Pentagonite, it is anything but strong in absolute terms. The energy difference between the ground state antiferromagnetic and ferromagnetic phases is barely 0.6 meV for Cavansite and 0.1 meV for Pentagonite. The approximate Curie temperature T_c can be computed using the formula

$$T_c = \frac{2J_{eff}}{3zk_B} = \frac{2\Delta E}{3zk_B}. \quad (1)$$

Here, the effective exchange constant (J_{eff}) is taken to be the difference ΔE in total

energies of the magnetic phases where z is the number of contributing magnetic atoms in the system ($z = 4$ in our case) and k_B is the Boltzmann constant. Using this, the T_c for the magnetic phase transition turns out to be, respectively, 1.32 K and 0.26 K for Cavansite and Pentagonite. This suggests that the magnetic vanadium ions interact extremely weakly with each other and, for all practical purposes, it would be difficult to experimentally detect any magnetic response in either of the minerals.

Energetically, Cavansite is seen to be lower by 0.26 eV per formula unit than Pentagonite. This can be attributed to their structural differences. Both the unit cells are characterized by sheets of Si-O₄ polyhedra in the **a-c** plane, stacked along the **c** axis. Also, the Si-O₄ polyhedra form rings when viewed along the longer **b** axis. Four water molecules per formula unit reside among the voids created by the sheets and the intermediate atoms of calcium and vanadium. However, a few more important differences in the structures of Cavansite and Pentagonite need to be highlighted. In Cavansite, calcium atoms have eight coordinating oxygen atoms: four from SiO₄ polyhedra and four from water. On the other hand, in Pentagonite the calcium atoms have seven oxygen atoms: four from SiO₄ polyhedra and only three from water, with the remaining water molecule hydrogen-bonded with other water molecules and oxygen atoms of silicate sheets. The polyhedral rings in Pentagonite are 6-membered rings while those in Cavansite are larger 8-membered rings joined via smaller 4-membered rings. This rearrangement is also associated with the restructuring of SiO₄ sheets. The reader may notice in Fig. 1 (bottom panel) that for Pentagonite the polyhedra are almost parallel (and anti-parallel) to each other, but for Cavansite they are tilted alternatively by 20° and 22.5°. This restructuring enables more compact packing (hence the reduction in volume) thereby lowering the ground-state energy of Cavansite.

From the ground-state energies, it is therefore reasonable to qualitatively expect that Cavansite will be more abundant than Pentagonite. Yet one cannot ignore the effect of pressure and temperature on their formation. This will be investigated below.

3.2. Temperature-dependent abundances

Approximate temperature-dependent abundances of a two-state system may be modeled using the following Boltzmann probability model:

$$p_i = \frac{e^{-E_i/k_B T}}{\sum_j e^{-E_j/k_B T}}, \quad (2)$$

where p_i is the probability of formation of state i (with $i, j \in \{\text{Cavansite}, \text{Pentagonite}\}$) at temperature T ; E_i is the energy of the state i ; and k_B is the Boltzmann constant. Because this is a two-state model, it follows that $p_{\text{Cavansite}} + p_{\text{Pentagonite}} = 1$.

The probability of formation of Pentagonite at zero pressure, computed as described, is shown in Fig. 4. As of today, it is not clear what the crystallization temperatures for Cavansite and Pentagonite in lava flows are, but as reported [7], Cavansite maintains crystallinity even when heated up to 670 K. The lava temperature at the time of formation is expected to be around or below this temperature and down to

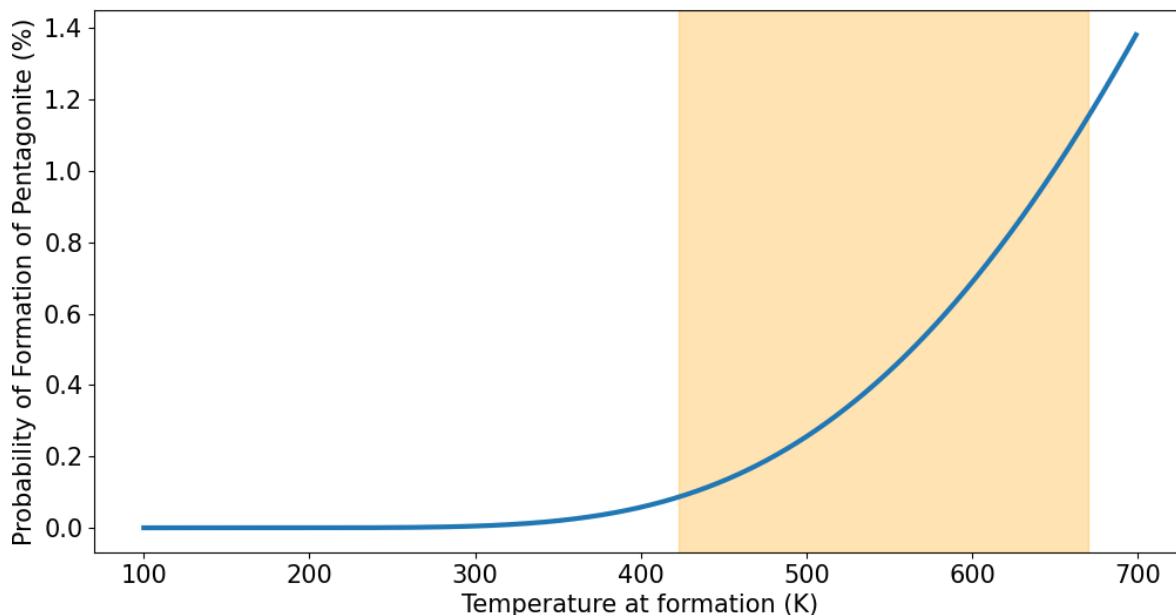


Figure 4. Probability for formation of Pentagonite as a function of temperature. The shaded area indicates a geophysically plausible range of crystallization temperatures.

450 K. For visualization purposes, this plausible regime of temperatures is highlighted in the figure. As seen in the figure, about 1% Pentagonite and 99% Cavansite is expected at around 650 K. In other words, for every 99 units of weight of Cavansite, one would find barely 1 unit weight of Pentagonite formed. These numbers might provide an insights as to why it is so difficult to find Pentagonite in the field.

A few caveats are in place here. The two-state Boltzmann probability model (Eq. 2) is a fairly simplistic view of what is arguably an extremely complex system of multiple interacting atomic and chemical units in a cooling-lava non-equilibrium environment. Specifically, this model assumes that there are no competing minerals during the formation of Cavansite and Pentagonite. While atomistic modeling of the cooling of a lava flow is practically impossible, it may be noted that the two-state Boltzmann probability model offers a useful first approximation.

3.3. Pressure-dependent abundances

To examine the effect of pressure on the formation of Cavansite and Pentagonite, we optimize the unit cells (anisotropically) at a specific target pressure. This is done by setting the target pressure and letting system vary the cell parameters and atomic positions so as to minimize the enthalpy. The enthalpy H is calculated at given pressure P and volumes V as:

$$H = E + PV, \quad (3)$$

where E is the total energy.

Fig. 5 presents the results of these optimizations including modified unit cell parameters and volumes normalized with respect to the ground state (i.e, at zero

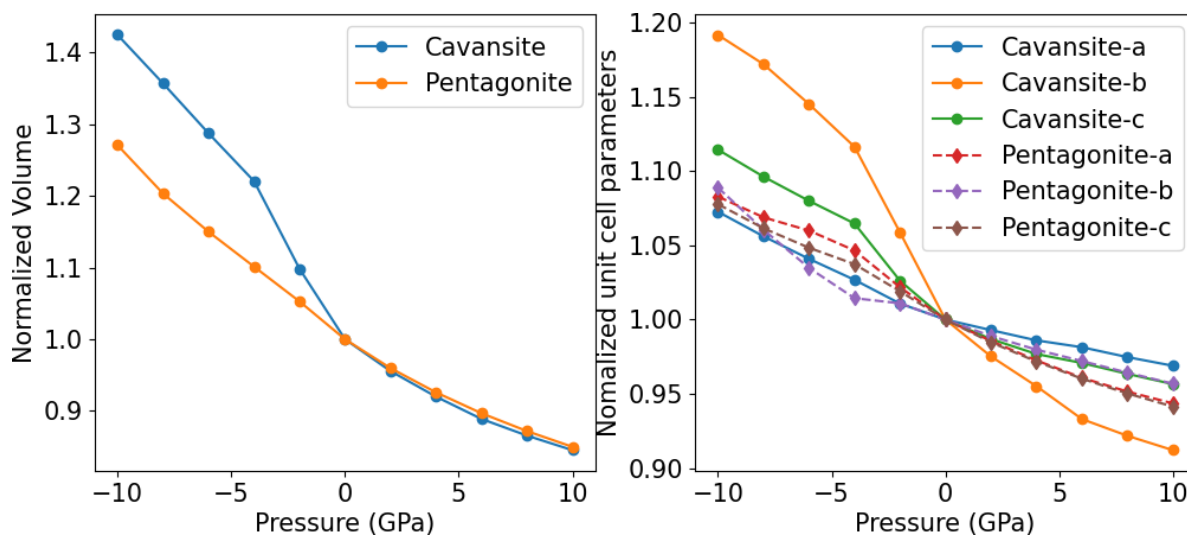


Figure 5. Evolution of (a) volume and (b) lattice parameters for Cavansite and Pentagonite as a function of pressure. Unit cell parameters for Pentagonite are shown by dashed lines to distinguish them from those of Cavansite. Note the somewhat drastic variations seen for Cavansite as compared to those for Pentagonite.

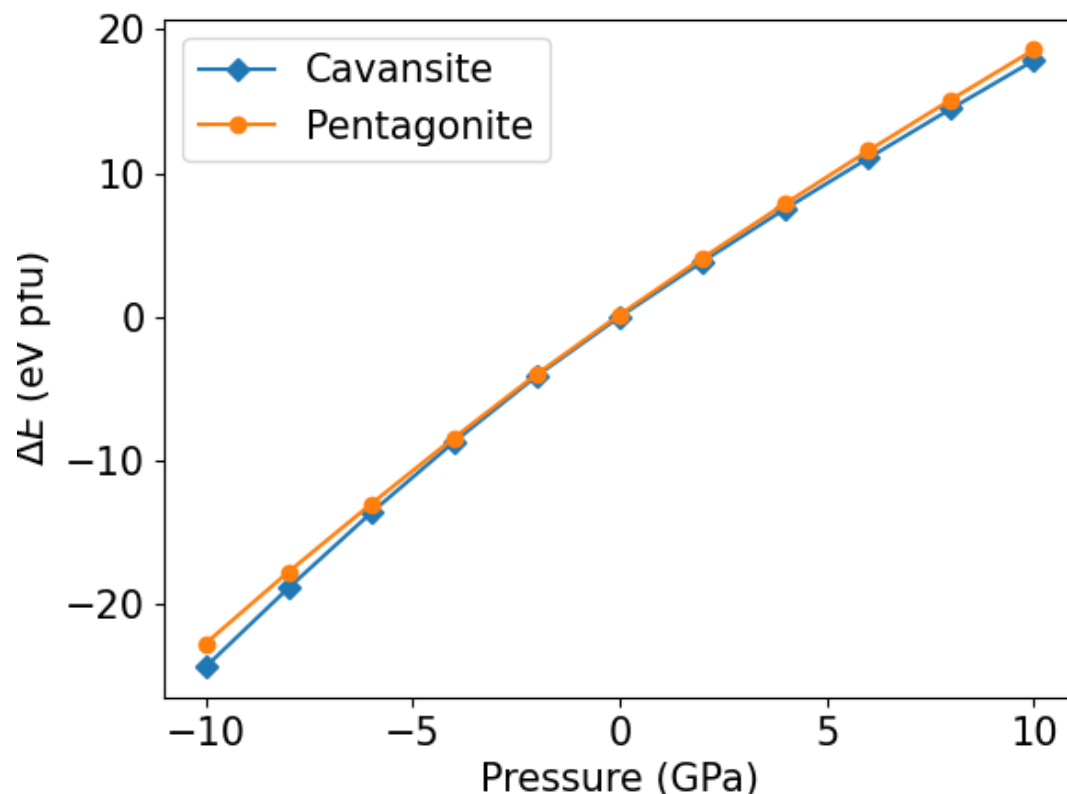


Figure 6. Variation of energies with pressure for both the systems. The zero is taken to be the ground state of Cavansite at zero pressure.

pressure). It illustrates the effect of pressure from -10 GPa to +10 GPa. It is worth noting that negative pressure (i.e., tensile strain or stretching of the unit cell) is of pure theoretical interest and is unlikely to be observed under geological conditions. It is evident from the results presented that the lattice structure of Cavansite experiences a significant change primarily driven by the variations along the **b** axis. Variations in unit cell of Pentagonite are relatively monotonous. This observation is consistent with the experimental finding by Danisi et al [21] (see Fig. 5 of the reference) who have noted similar anisotropic compressibility along the **b** axis only for Cavansite.

The fact that Pentagonite displays less compressibility along all axes suggests a high bulk modulus. The bulk modulus is computed by fitting the Birch-Murnaghan equation-of-state [22] to the volume-energy data. Fig. 6 shows the energies (with respect to the ground state energy of Cavansite at zero pressure) as functions of volume. From these data, bulk moduli are estimated to be 33.7 GPa and 41.1 GPa for Cavansite and Pentagonite respectively. These numbers are in excellent agreement with those observed experimentally (38 GPa and 49 GPa respectively) [21]. Importantly, for all positive pressures, Cavansite remains lower in energy (hence favored).

3.4. Pressure-temperature (*P-T*) phase diagram of abundances

Sec. 3.2 and 3.3 examine the effects of pressure and temperature separately. Here, they are combined into a *P-T* phase diagram. Using Eq 2, we compute probabilities for a range of temperatures and pressures for both the systems. The resulting phase diagram is shown in Fig. 7. Here, colors indicate the probabilities of formation of the two species, and contours corresponding to 99%, 95% and 90% probabilities of formation of Cavansite are overlaid on the plot as visual guide. We see that Cavansite dominates the phase diagram for most part. Because probabilities $p_{\text{Cavansite}} + p_{\text{Pentagonite}} = 1$ in our model (Sec. 3.2), these contours also indicate the 1%, 5% and 10% probabilities of formation of Pentagonite. Clearly, pressure and temperature both appear to aid the formation of Pentagonite – however so slightly – with the effect becoming less and less prominent at higher pressures. (As noted before, negative pressures are unlikely under geological conditions of formation of these minerals.) It appears that there may be fairly narrow window in the *P-T* plane which favours the formation of Pentagonite.

Ishida et al [20] note that Pentagonite is a high-temperature polymorph of Cavansite. This is consistent with the results of the present analysis. A higher probability requires even higher temperatures. In other words, presence of Pentagonite in the lava flow cavities might suggest either higher lava or fluid temperatures for substantial duration.

3.5. Dehydration of crystals

The role of water molecules in the structure is now investigate by removing one water molecule at a time and then performing full unit cell relaxations. For each level of (de)hydration, multiple different unit cell configurations are possible. Specifically, for *k*

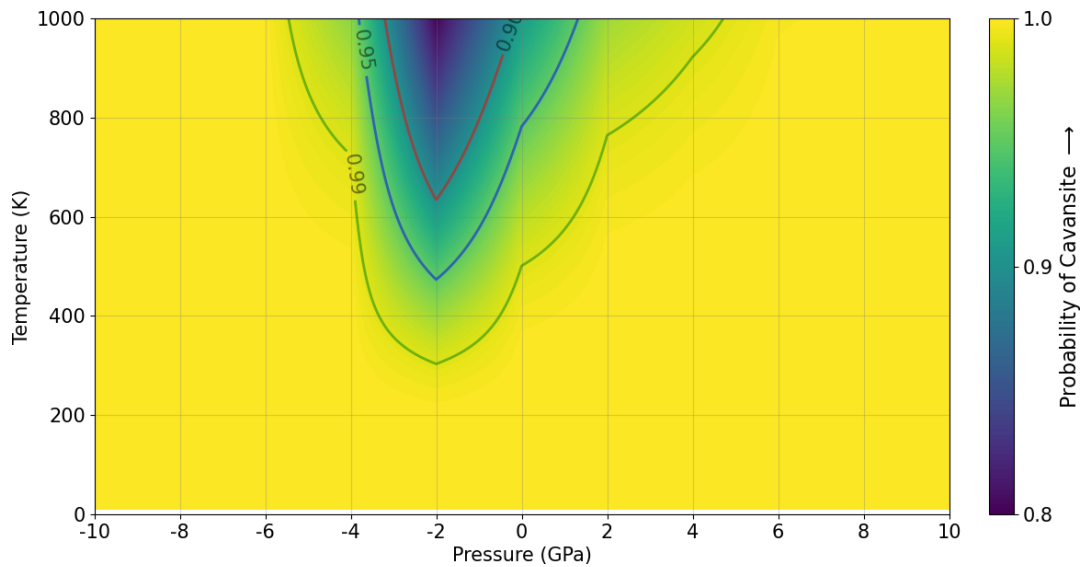


Figure 7. Probability of formations of Cavansite and Pentagonite (see the color axis) as a function of pressure (x axis) and temperature (y axis). Yellow color indicates the 100% probability of formation of Cavansite. Three contours corresponding to 99% (green), 95% (blue) and 90% (red) formation probability of Cavansite are shown as visual aid.

	a	b	c	$\Delta V(\text{\AA}^3)$	Reported $\Delta V(\text{\AA}^3)$ [7]
Cavansite	9.940	12.944	9.764		
25% dehydrated Cavansite	9.724	13.404	9.606	-4.2	-6.19
50% dehydrated Cavansite	9.577	12.782	9.472	-96.8	-82.03
75% dehydrated Cavansite	9.309	12.557	9.358	-162.3	-132.92
Dehydrated Cavansite	8.960	12.102	9.046	-275.4	
Pentagonite	10.093	14.475	8.838		
25% dehydrated Pentagonite	10.034	14.006	8.850	-47.8	
50% dehydrated Pentagonite	10.026	13.863	8.905	-53.6	
75% dehydrated Pentagonite	9.932	13.256	8.726	-142.4	
Dehydrated Pentagonite	10.012	12.318	9.032	-177.3	

Table 2. Cell parameters of Cavansite and Pentagonite at different values of dehydration. The change in volumes (ΔV) with respect to the fully hydrated cell is also shown. Additionally last column shows the experimentally available values of ΔV .

water molecules per unit cell, there can be $\binom{4}{k}$ unit cell configurations ($k = 0, \dots, 4$). All the configurations for each k are systematically generated and fully optimized. Reported here are only the ones with the lowest energy. See Table 2 for our optimized cell parameters and a comparison with experimentally available values[7]. The reader may note that the unit cell volume decreases with the removal of water. This is expected and indicates the reduction in volume of the voids inside a unit cell. These results are consistent with experimentally available values including the drastic reduction in

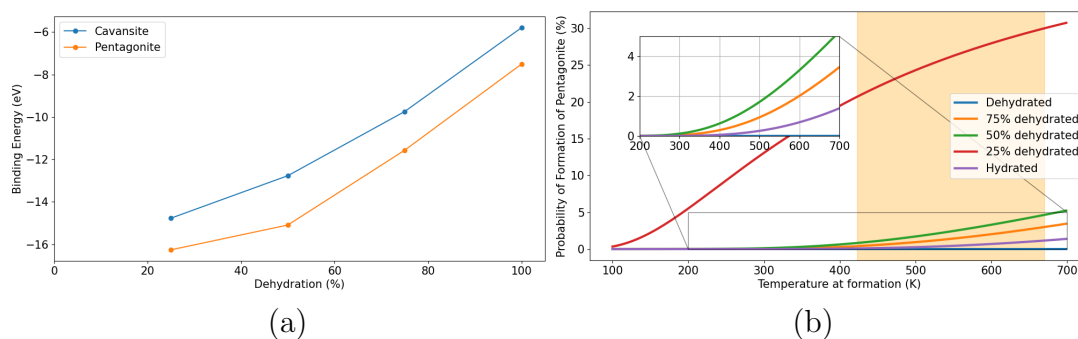


Figure 8. (a) Binding energies of water molecules as a function of dehydration. We note relative flattening of the Pentagonite curve (orange) at the lowest value of dehydration signifying the relatively less resistance for the removal of water. (b) Relative abundance for Pentagonite as a function of dehydration.

Cavansite volume from 25% to 50%. However, note that the experimental values are obtained at significantly high temperatures – a factor that cannot be easily incorporated in the present results. Overall, it is seen that Cavansite undergoes a more dramatic volume loss compared to Pentagonite.

Fig. 8(a) shows binding energies of water at individual step of dehydration. Although Cavansite as a whole has overall lower energy, the individual water molecules have less binding energy than those in Pentagonite. This is true irrespective of the level of dehydration. We also see nearly monotonous reduction in binding for Cavansite upon increasing levels of dehydration. It is to be noted that Pentagonite shows a slight flattening of the curve at 25% of dehydration. This is because, as explained before, calcium in Cavansite forms octahedra which harbour all four water molecules, in contrast to Pentagonite for which one of water molecule is not bound to calcium octahedra. As a result, it is relatively easy to remove the first water molecule in Pentagonite than other rest three. This amounts to reduction in the overall energy difference between Cavansite and Pentagonite which is further reflected in the abundance curves (Fig. 8 (b)). As seen from the figure – except for 25% dehydration – the probability of formation of Pentagonite follows a similar exponential trend as in Fig. 4. However, the probability of formation increases with dehydration. This increase is drastic at 25% dehydration due the reason mentioned above. Overall, one might conjecture that water-stressed environment might lead to a higher abundance of Pentagonite. Yet, there is no evidence from the field data that indicates any insufficient inclusion of water molecules in these crystals. Samples reported in the literature seem to indicate complete hydration.

At this point, the role of van der Waals (vdW) interaction is worth a note. Without vdW corrections, it is known that DFT calculations overestimate typical cell lengths by about 10% compared to uncorrected calculations. This is, of course, expected because non-vdW-corrected DFT functionals do not accurately capture the long-range attractive vdW interaction. In the present context, it is seen that in absence of the vdW correction, the ground state energy of dehydrated Pentagonite is lower than that of dehydrated

Cavansite. On the other hand, vdW-corrected calculations predict that Cavansite is the energetically more favourable ground state structure. A conclusive resolution of this issue may be possible only through experiments.

4. Implications of our results to mineralisation

The computational analysis and results presented in this paper may have interesting implications to the current understanding of the mineralisation processes leading to the formation of Cavansite and Pentagonite. This is elaborated upon below.

Wagholi, Pune, India, is the seat of currently the largest deposits of both Cavansite and Pentagonite. Here, a thick (~ 10 m), massive basaltic lava flow is exposed and is quarried for road metal and aggregates. At its base, its contact with the lower lava flow is marked by sporadic patches of flow-top breccia. This highly oxidized, glassy breccia has high porosity and permeability with copious irregular and haphazard vugs and cavities containing heulandite, stilbite, a rare green apophyllite, and two generations of calcite. Radiated aggregates or sheaf-like crystals of Cavansite grow on top of heulandite, stilbite and calcite. In 1998, the rarer Pentagonite was discovered to co-occur with its diamorph Cavansite in some of the cavities [23]. Cavansite and Pentagonite occurrences at Wagholi are characterized by high vanadium concentrations of 600-750 ppm in the host basalts [24]. Thus, the presence of vanadium-bearing minerals suggests in situ scavenging of vanadium from glassy basalt by hydrothermal fluids and their subsequent deposition in micro niche environments [25].

The findings of the present study suggest the following possibilities about the mineralisation processes that lead to the formation of Cavansite and Pentagonite.

- (i) It is speculated that Cavansite may have been deposited first by hydrothermal fluids under saturated conditions (which is a common process for zeolite formation in cavities over relevant geological time scales). Pentagonite got deposited only after the temperature in the cavities rose and evaporated the fluid in the cavities at slightly faster rates (explaining relatively small crystal sizes). The top layer of lava mentioned earlier could be one possible reason for temperature rise in the lower layer because of blanketing of the lower layer.
- (ii) The observed abundances of Cavansite and Pentagonite are explained through two mechanisms which may act separately or in tandem under geological conditions:
 - (a) Through the fundamental physics of these two minerals leading to the probabilities presented earlier ($\sim 1\%$ for Pentagonite and $\sim 99\%$ for Cavansite in the relevant lava temperature range of 450-650 K. It is speculated that the thick lava flows from Wagholi might have cooled under a similar thermal regime (perhaps even lower) when zeolite mineralisation was initiated in the breccia cavities.

One must also remember that breccia are known to experience considerable overburden pressure in addition to the fluid pressure in the cavities. In the

P-T phase diagram (Fig. 7), there is a distinct area around 4 GPa at high enough temperatures where we see a significant probability of formation of Pentagonite. However, these conditions are rarely achieved in real-life lava flows. Consequently, the probability of formation of Pentagonite remains significantly low despite higher temperatures.

- (b) Via the normal geological spatiotemporal variability of prevailing temperature and pressure conditions, suggesting that only a limited fraction of vugs and cavities may have been exposed to appropriate temperature, pressure and chemical conditions favouring the formation of Pentagonite.

5. Conclusion

In this work, extensive DFT calculations have been performed to examine the electronic structures, structural properties, and relative abundances of two microporous vanadosilicate dimorphs, namely Cavansite and Pentagonite. This analysis finds that the structural arrangements of SiO_4 tetrahedra as well as the differently-coordinated calcium atoms are responsible for the lower ground state energy of Cavansite at zero pressure and zero temperature. The analysis also computes electronic structures under pressure to mimic field conditions in the lava flows where these minerals are formed. A two-state Boltzmann probability model is used to model the effect of temperature on the relative abundances of the two minerals. This leads to the construction of a comprehensive pressure-temperature-abundance phase diagram for the two minerals. This phase diagram explains why Cavansite is significantly more abundant than Pentagonite. This analysis further suggests that the formation of Pentagonite is assisted by both pressure and temperature although this effect is most pronounced over a limited range of (negative) pressures. This study provides insights into mineralization processes that lead to or contribute to the deposition of Cavansite and Pentagonite in the observed proportions. The DFT calculations presented here also predict a highly localized weak magnetic state due to vanadium atoms that is associated with weak magnetic ordering at very low temperatures (Curie temperatures around 1 K). Hydration in both the minerals is investigated, and indicates that water molecules are somewhat loosely bound to the crystal structure. This work sheds light on both for the geological and material science aspects of vanadosilicate minerals and paves way for further studies of their formation and properties.

Acknowledgments

BSP thanks Andrey Tokarev for valuable comments.

Competing Interests None

References

- [1] Staples L W, Evans Jr H T and Lindsay J R 1973 *American Mineralogist: Journal of Earth and Planetary Materials* **58** 405–411
- [2] Evans Jr H T 1973 *American Mineralogist: Journal of Earth and Planetary Materials* **58** 412–424
- [3] Ottens B, Schuster R and Benkó Z 2022 *Minerals* **12** 444
- [4] Huang H M, Shih Y H, Chen H F, Lee H Y, Fang J N, Shen C C and Yu B S 2023 *Minerals* **13** 1221
- [5] Danisi R M, Armbruster T, Arletti R, Gatta G D, Vezzalini G, Quartieri S and Dmitriev V 2015 *Microporous and Mesoporous Materials* **204** 257–268 ISSN 1387-1811 URL <https://www.sciencedirect.com/science/article/pii/S1387181114006799>
- [6] Phadke A V and Apte A 1994 *Mineralogical Magazine* **58** 501–505
- [7] Danisi R M, Armbruster T and Lazic B 2012 *American Mineralogist* **97** 1874–1880
- [8] Cymes B A 2020 *Catalytic Properties of Novel Microporous Minerals* Ph.D. thesis Miami University
- [9] Srivastava S, Dong H, Baars O and Sheng Y 2023 *Geobiology*
- [10] Sheng Y, Baars O, Guo D, Whitham J, Srivastava S and Dong H 2023 *Environmental Science & Technology* **57** 7206–7216
- [11] White J S 2002 *Rocks & Minerals* **77** 274–275
- [12] Perdew J P, Burke K and Ernzerhof M 1996 *Physical review letters* **77** 3865
- [13] Giannozzi P, Baroni S, Bonini N, Calandra M, Car R, Cavazzoni C, Ceresoli D, Chiarotti G L, Cococcioni M, Dabo I *et al.* 2009 *Journal of physics: Condensed matter* **21** 395502
- [14] Garrity K F, Bennett J W, Rabe K M and Vanderbilt D 2014 *Computational Materials Science* **81** 446–452
- [15] Dal Corso A 2014 *Computational Materials Science* **95** 337–350
- [16] Kucukbenli E, Monni M, Adetunji B, Ge X, Adebayo G, Marzari N, De Gironcoli S and Corso A D 2014 *arXiv preprint arXiv:1404.3015*
- [17] Lejaeghere K, Bihlmayer G, Björkman T, Blaha P, Blügel S, Blum V, Caliste D, Castelli I E, Clark S J, Corso A D, de Gironcoli S, Deutsch T, Dewhurst J K, Marco I D, Draxl C, Dulak M, Eriksson O, Flores-Livas J A, Garrity K F, Genovese L, Giannozzi P, Giantomassi M, Goedecker S, Gonze X, Grånäs O, Gross E K U, Gulans A, Gygi F, Hamann D R, Hasnip P J, Holzwarth N A W, Iuşan D, Jochym D B, Jollet F, Jones D, Kresse G, Koepernik K, Küçükbenli E, Kvashnin Y O, Locht I L M, Lubeck S, Marsman M, Marzari N, Nitzsche U, Nordström L, Ozaki T, Paulatto L, Pickard C J, Poelmans W, Probert M I J, Refson K, Richter M, Rignanese G M, Saha S, Scheffler M, Schlipf M, Schwarz K, Sharma S, Tavazza F, Thunström P, Tkatchenko A, Torrent M, Vanderbilt D, van Setten M J, Speybroeck V V, Wills J M, Yates J R, Zhang G X and Cottenier S 2016 *Science* **351** aad3000 (*Preprint* <https://www.science.org/doi/pdf/10.1126/science.aad3000>) URL <https://www.science.org/doi/abs/10.1126/science.aad3000>
- [18] Prandini G, Marrazzo A, Castelli I E, Mounet N and Marzari N 2018 *npj Computational Materials* **4** 72
- [19] Grimme S, Antony J, Ehrlich S and Krieg H 2010 *The Journal of Chemical Physics* **132** 154104 (*Preprint* <https://doi.org/10.1063/1.3382344>) URL <https://doi.org/10.1063/1.3382344>
- [20] Ishida N, Kimata M, Nishida N, Hatta T, Shimizu M and Akasaka T 2009 *Journal of mineralogical and petrological sciences* **104** 241–252
- [21] Danisi R M, Armbruster T, Arletti R, Gatta G D, Vezzalini G, Quartieri S and Dmitriev V 2015 *Microporous and Mesoporous Materials* **204** 257–268
- [22] Birch F 1947 *Phys. Rev.* **71**(11) 809–824 URL <https://link.aps.org/doi/10.1103/PhysRev.71.809>
- [23] Ottens B, Blass G and Graf H 2000 *Mineralien-Welt* **2** 59–62
- [24] Ghodke S, Powar K and Kanegoankar N 1984 Trace elements distribution in deccan trap flows in dive ghat area, pune district, maharashtra *Proc. Symp. on Deccan Traps and Bauxites, Geological*

Survey of India. Special Publication 14 pp 55–62

- [25] Ottens B 2003 *The Mineralogical Record* **34** 5–83
 [26] Birch W 1977 *Mineralogical Record* **8** 61–62
 [27] Kothavala R 1991 *The Mineralogical Record* **22** 415–420
 [28] Cook R B 1996 *Rocks & Minerals* **71** 180–182
 [29] Powar K and Byrappa K 2001 *Journal of Mineralogical and Petrological Sciences* **96** 1–6
 [30] Makki M F 2005 *Mineralogical Record* **36** 507
 [31] Mookherjee A and Phadke A 1998 *Gondwana Geological Magazine* **13** 23–27
 [32] Praszker T and Siuda R 2007 *Mineralogical Record* **38** 185
 [33] Praszker T 2009 *Mineralien-Welt* **20** 16
 [34] Frank H, Alegre P and Thornton J 2004 *Mineralien magazin lapis* 41–42

Appendix

Locality	Lava type	Host locale	Mineral association	Reference
Columbia River Flood Basalt Province, USA				
Qwyhee Dam, Oregon	Rhyolite, tuff breccia intruded by dyke	Red tuff breccia	Cavansite, heulandite, stilbite, calcite, apophyllite, analcime, rare pentagonite, native copper	Staples et al.[1]
Charles W. Chapman quarry, Goble, Oregon	Rubbly pahoehoe intruded by dykes	Cavity filling, calcite veins	Cavansite, calcite, heulandite, thomsonite, native copper	Staples et al.[1]
Deccan traps, India				
Wagholi, Pune	Rubbly pahoehoe	Flow top breccia (FTB)	Cavansite, Pentagonite, stilbite, mordenite, heulandite, calcite, apophyllite, native copper	Evans [2], Birch [26], Kothvala [27]; Cook [28], Blass et al. [23], Powar and Byrappa[29]; Ottens [25], Makki [30]
Sutarwadi, Pune	Sheet pahoehoe	Gas blister	Cavansite, stilbite	Mookherjee and Phadke [31]
Yedgaon Dam, Narayangaon	Sheet pahoehoe	Cavity filling	Cavansite	Mookherjee and Phadke [31]

Surli Ghat, Karad	Rubbly pahoehoe	FTB	Cavansite	Mookherjee and Phadke [31]
Lonavala Quarry	Sheet pahoehoe	Cavity filling	Cavansite, calcite, heulandite-Ca, modernite, pentagonite, quartz	Praszkier and Siuda, [32]
Indori, Talegaon	Sheet pahoehoe	Cavity filling	Cavansite, stilbite, apophyllite, mesolite, modernite, heulandite, calcite	Praszkier, [33]
Rio Grande do Sul, Brazil				
Morro Reuter, Brazil	Vesicular basalt	Vein filing	Cavansite, quartz	Frank et al., 2004 [34]
New Zealand				
Aranga Quarry, Dargaville	likely Rubbly pahoehoe	Red breccia	Cavansite, chabazite-Ca, calcite, okenite, native copper, chrysocolla	Frank et al [34]

Table A1: Locations and details of the conditions where Cavansite and Pentagonite are found across the world. There are only a handful of basaltic planes where they are found with the best known specimens emerging from Pune, India.